



Truncated string state space approach and its application to the nonintegrable spin- $\frac{1}{2}$ Heisenberg chain

Jiahao Yang (杨家豪)¹ and Jianda Wu (吴建达)^{1,2,3,*}

¹*Tsung-Dao Lee Institute, Shanghai Jiao Tong University, Shanghai 201210, China*

²*School of Physics and Astronomy, Shanghai Jiao Tong University, Shanghai 200240, China*

³*Shanghai Branch, Hefei National Laboratory, Shanghai 201315, China*



(Received 17 January 2024; revised 11 April 2024; accepted 31 May 2024; published 14 June 2024)

By circumventing the difficulty of obtaining exact string state solutions to Bethe ansatz equations, we devise a truncated string state space approach for investigating spin dynamics in a nonintegrable spin- $\frac{1}{2}$ Heisenberg chain subjected to a staggered field at various magnetizations. The obtained dynamical spectra reveal a series of elastic peaks at integer multiples of the ordering wave vector Q , indicating the presence of multi- Q Bethe string states within the ground state. The spectrum exhibits a separation between different string continua as the strength of the staggered field increases at low magnetization, reflecting the confinement of the Bethe strings. This approach provides a unified string-state-based framework for understanding spin dynamics in low-dimensional nonintegrable Heisenberg models, which has a successful application to observations across various phases of the quasi-one-dimensional antiferromagnet YbAlO_3 .

DOI: [10.1103/PhysRevB.109.214421](https://doi.org/10.1103/PhysRevB.109.214421)

I. INTRODUCTION

One-dimensional quantum systems characterized by exact solutions and quantum integrability offer a fascinating arena to study many-body physics. Notable examples include the one-dimensional (1D) spin- $\frac{1}{2}$ XXZ model [1–4], Gaudin-Yang model [5–7], Lieb-Liniger model [8,9], and quantum Ising models [10–13]. Although these models have paved the way for determining the eigenstates and eigenenergies of those systems, it has long been a challenge to calculate their form factors and thus dynamical response, which was partly tackled recently [7,14–20]. Empowered by the theoretical development, the spin dynamics of celebrated many-body quasiparticles, such as spinons [21–23], strings [24–26], and E_8 [27–31] and $D_8^{(1)}$ particles [32–34], have been extensively explored, providing crucial guidance for experimental observations in quasi-1D materials [3,30,31,35–40]. This progress has led to the cooperative effort of both theorists and experimentalists to unveil the intricate nature of these exotic phenomena.

Bearing real materials in mind, it becomes crucial to ask how robust integrable physics is against nonintegrable perturbations that may partially or fully break the conservation laws of integrable systems. This has inspired extensive research focused on nonintegrable models such as spin- $\frac{1}{2}$ ladders [41,42], chains with a staggered magnetic field [43,44], frustrated spin chains [45], and dimerized spin chains [46,47]. Most studies are performed using effective field theory [43,44] or numerical methods such as the exact diagonalization (ED) [45,46], matrix product state [47], and quantum Monte Carlo methods [48]. However, on the one hand, numerical methods in general

lack a clear understanding of the essential physical picture; on the other hand, the effective field theory can provide only limited insight within the low-energy and long-wavelength limit. Therefore, a method able to go beyond those limitations is always desired.

At first glance it may seem promising to apply Bethe states to study nonintegrable systems. However, a notorious open problem persists: finding the precise *complex* solutions of the Bethe ansatz equation (BAE) for string states [24,49–53]. In the past few decades, many approaches have been explored, including a carefully designed iterative method [54] and a rational Q -system method [55–57]. The former can easily access large system size but suffers from many unphysical solutions with repeated roots. Although the latter can solve the BAE for all exact solutions simultaneously, it is limited to a small system size. Those shortcomings impede the practical application of Bethe states to understand nonintegrable systems of reasonable size.

In this paper, we first outline a solving machine for the spin- $\frac{1}{2}$ Heisenberg chain which can obtain exact solutions for Bethe string states. Based on these string states, we develop a truncated string state space approach (TS³A) to study a nonintegrable Hamiltonian, specifically the spin- $\frac{1}{2}$ Heisenberg chain with a staggered field. The TS³A can determine the eigenstate and eigenenergy for the nonintegrable Hamiltonian in the truncated Hilbert space. Additionally, we evaluate its efficiency for small systems under various truncation schemes involving different energy cutoffs and string lengths by comparing its performance to that of ED calculations.

Following the TS³A, we analyze the nonintegrable spin dynamics in the spin- $\frac{1}{2}$ Heisenberg chain with staggered field characterized by wave vector Q . In addition to the Q ordering of the system, a series of elastic peaks appears at nQ ($|n| = 2, 3, \dots$), indicating the ground state contains multi- Q Bethe

*Contact author: wujd@sjtu.edu.cn

string states. Moreover, the staggered field plays the role of the confining field for the Bethe string states, constraining the motion of spins along the chain. The confinement of Bethe strings results in two separated continua in dynamical spectra at low magnetization. Notably, the above results were successfully applied to experimental observations of the quasi-1D antiferromagnet YbAlO_3 , aligning with the unified Bethe-string-based framework provided by the TS^3A [58].

The rest of this paper is organized as follows. Section II introduces the Hamiltonian of the 1D Heisenberg model with a staggered field. Section III illustrates the Bethe string state and then presents a method for obtaining exact solutions from the BAE. The framework of the TS^3A is developed, and its efficiency is investigated in Sec. IV. Then Sec. V discusses the spin dynamics of the nonintegrable Hamiltonian. Section VI contains the conclusion and outlook.

II. MODEL

Our parent Hamiltonian is the 1D Heisenberg spin- $\frac{1}{2}$ model with longitudinal field h_z ,

$$H_0 = J \sum_{n=1}^N \mathbf{S}_n \cdot \mathbf{S}_{n+1} - h_z S_n^z, \quad (1)$$

with N being the total number of sites, J being antiferromagnetic coupling, and \mathbf{S}_n being spin operators with components S_n^μ ($\mu = x, y, z$) at site n . With the introduction of a staggered field $\mathbf{h}_Q = h_Q \sum_i \cos(Qr_i) \hat{z}$ which couples to the spin chain, the total Hamiltonian becomes nonintegrable,

$$H = H_0 + H', \quad (2)$$

where

$$H' = - \sum_n \mathbf{h}_Q \cdot \mathbf{S}_n = -h_Q \sum_n \cos(Qr_n) S_n^z. \quad (3)$$

h_Q is the strength of the staggered field, and the ordering wave vector $Q = (1 - m)\pi$, where the magnetization density $m = M_z/M_s$, which is the ratio of magnetization M_z to its saturation value M_s . In practice, the staggered field can be effectively induced from three-dimensional (3D) magnetic ordering of quasi-1D materials, such as YbAlO_3 [58–61], $\text{SrCo}_2\text{V}_2\text{O}_8$ [62], and $\text{BaCo}_2\text{V}_2\text{O}_8$ [30]. We note that the staggered field can be both commensurate and incommensurate, depending on whether $2\pi/Q$ is a rational or irrational number, respectively.

III. EXACT BETHE STRING STATE

In this section, we begin with an introduction to the coordinate Bethe ansatz and Bethe string states for the Hamiltonian H_0 [Eq. (1)]. Then an efficient method is presented for obtaining the exact solutions from the BAE.

A. Bethe ansatz and the Bethe string state

Due to $U(1)$ symmetry of H_0 [Eq. (1)] the magnetization $M_z = 1/2 - M/N$ is the conserved quantity, where M is the number of down spins, i.e., magnons, with respect to the fully polarized state with all up spins $|\uparrow \cdots \uparrow\rangle$. In the coordinate Bethe ansatz [63–65], the eigenstate of H_0 [Eq. (1)] is the

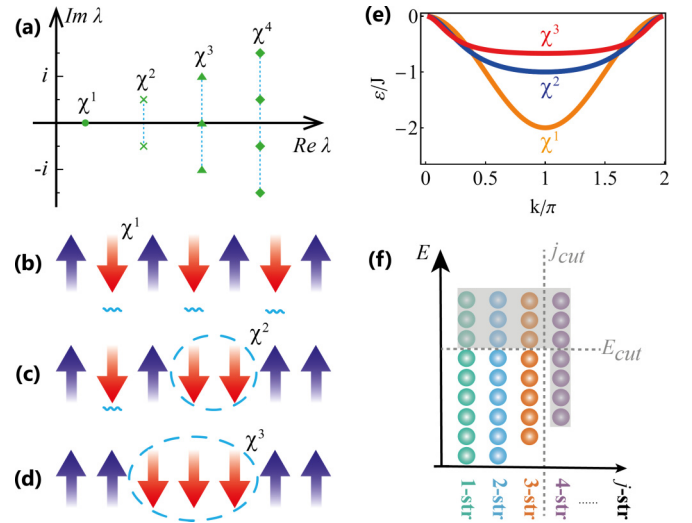


FIG. 1. (a) The rapidities of Bethe strings with different lengths in the complex plane. (b)–(d) Pictorial spin configurations of the Bethe strings. View the down spin (red arrows) and up spin (blue arrows) as the magnon and vacuum, respectively. A single Bethe string χ^j contains j bounded magnons. (e) The energy-(quasi)momentum relation for Bethe strings χ^j . (f) Illustration of the truncated string state space, where each ball denotes a j -string state. The shaded region is separated by vertical and horizontal lines representing the cutoffs for string length and the energy, respectively.

Bethe state with M magnons, which is determined by a set of rapidities $\{\lambda_l\}_M$ satisfying the BAE,

$$\left(\frac{\lambda_l + i/2}{\lambda_l - i/2} \right)^N = \prod_{k \neq l} \left(\frac{\lambda_l - \lambda_k + i}{\lambda_l - \lambda_k - i} \right), \quad (4)$$

with $l = 1, \dots, M$. The corresponding quasimomentum $k_l = \pi - 2 \arctan(2\lambda_l)$. These rapidities $\{\lambda_l\}_M$ manifest as either complex-conjugate pairs or real numbers [Fig. 1(a)] [66]. The pair of complex rapidities implies a significant physical property: the corresponding magnons exhibit an intriguing phenomenon in coordinate space, forming effectively bounded magnons commonly known as a “Bethe string” [24,64,67]. And the length of the string is determined by the number of rapidities with a common real center. Intuitively, Bethe string χ^j ($j \geq 2$) of length j is a “big” quasiparticle in which j bounded magnons move coherently, referred to as a j -string [Figs. 1(b)–1(d)]. When $j = 1$, the 1-string χ^1 is just the unbound magnon. Correspondingly, the rapidities of a string χ^j take the form [24,49]

$$\lambda_{j,\alpha}^n = \lambda_{j,\alpha} + \frac{i}{2}(j+1-2n) + d_{j,\alpha}^n, \quad (5)$$

where $n = 1, \dots, j$ denotes the j th magnon in the j -string. The number of j -strings is denoted as M_j , and $\alpha = 1, \dots, M_j$ label different j -strings with the same length j . Thus, we have $\sum_j j M_j = M$ for an M -magnon Bethe state. We refer to $\lambda_{j,\alpha}$ as the string center, which gives the real part of the j -string if the deviation $d_{j,\alpha}^n$ is omitted. Under the assumption $d_{j,\alpha}^n = 0$, we obtain the eigenenergy of a Bethe string state, $E = \sum_{j,\alpha} \varepsilon_{j,\alpha}$, with $\varepsilon_{j,\alpha} = -2jJ/(4\lambda_{j,\alpha}^2 + j^2)$. Therefore, we can show the relation between energy and quasimomentum for

TABLE I. The solutions of a 3-string state to Bethe ansatz equation (4) with $N = 12$ and $M = 5$. The solutions presented in the first row are obtained with the method in Ref. [54], while those in the second row are obtained with our method. Note that in the first row, λ_3^3 and λ_1^1 coincide, indicating an unphysical outcome.

	λ_3^1	λ_3^2	λ_3^3	λ_1^1	λ_1^2
Unphysical	$0.4955 + 0.9622i$	$0.4955 - 0.9622i$	0.4458	0.4458	0.1803
Physical	$0.4918 + 0.9615i$	$0.4918 + 0.9615i$	$0.4448 + 0.0188i$	$0.4448 - 0.0188i$	0.1807

different strings in Fig. 1(e). For finite $d_{j,\alpha}^n$, the eigenenergy becomes $E = \sum_{j,\alpha,n} \varepsilon_{j,\alpha}^n$, with $\varepsilon_{j,\alpha}^n = -2J/[4(\lambda_{j,\alpha}^n)^2 + 1]$.

To ensure clarity in terminology, we refer to a Bethe state with all M magnons being χ^1 as the 1-string state. For $j > 1$, we classify an $n * j$ -string state with $M_j = n$ and $M_1 = M - n * j$. When $n = 1$, it is simply referred to as the j -string state. This convention can be consistently extended to cover other cases.

B. Exact solution

To characterize Bethe string states, the initial step is to obtain rapidities $\{\lambda_j\}$ ($j = 1, \dots, M$) by solving the BAE [Eq. (4)]. This is commonly achieved by considering the logarithmic form of the BAE,

$$\frac{2\pi}{N} I_j = \Theta_1(\lambda_j) - \frac{1}{N} \sum_{k=1}^M \Theta_2(\lambda_j - \lambda_k), \quad (6)$$

where $\Theta_j(\lambda) = 2 \arctan(2\lambda/j)$ and I_j is the corresponding Bethe quantum number. Equation (6) is highly efficient for finding the real solutions using the iterative method [54,68]. However, for complex solutions, we first need to consider the reduced Bethe equation with $d_{j,\alpha}^n \rightarrow 0$ [67],

$$\frac{2\pi}{N} I_{j,\alpha} = \Theta_j(\lambda_{j,\alpha}) - \frac{1}{N} \sum_{k=1}^M \sum_{\substack{\beta=1 \\ (k,\beta) \neq (j,\alpha)}}^{M_k} \Theta_{jk}(\lambda_{j,\alpha} - \lambda_{k,\beta}) \quad (7)$$

$\forall j$ with $M_j \neq 0$ and $\alpha = 1, \dots, M_j$, with $\Theta_n(\lambda) = 2 \arctan(2\lambda/n)$ and $\Theta_{nm} = (1 - \delta_{nm})\Theta_{|n-m|} + 2\Theta_{|n-m|+2} + \dots + 2\Theta_{n+m-2} + \Theta_{n+m}$. $I_{j,\alpha}$ is referred to as the reduced Bethe quantum number. Equation (7) can also be tackled iteratively to obtain the string centers $\{\lambda_{j,\alpha}\}$, whose associated complex solutions are constructed from Eq. (5) with $d_{j,\alpha}^n = 0$. Nevertheless, these solutions are generally not exact because they disregard the finite deviation $d_{j,\alpha}^n$. By utilizing the solutions obtained with Eq. (7) as an initial guess, the finite deviation is accessible for a majority of the string states following the method in Ref. [54]. A summary is presented in Appendix A.

However, the strategy introduced above fails to generate all exact solutions when the number of lattice sites exceeds $N \gtrsim 12$ (see the example in Table I and details in Appendix A). The limitations arise from the generation of repeated real rapidities in string states which are physically forbidden [69,70]. The key to solving this problem is that the repeated real rapidities actually form a complex-conjugate pair with a minor imaginary part (typically, $\lesssim 1/N$). To implement the observation in the algorithm, we divide and conquer; the details are given in Sec. A 3. For instance, for a 3-string state, the typical rapidity

pattern is that three of them share a common real part up to a finite deviation $d_{j,\alpha}^n$, while the remaining rapidities are all real. However, when we encounter repeated real rapidities (see the first row of Table I), usually involving the 3-string center and one real rapidity, we introduce a small imaginary part to create a complex-conjugate pair. This pair and other rapidities are then treated as a new initial guess for the BAE, from which we are able to efficiently obtain the exact solution (the second row in Table I).

Before ending this section, it is imperative that we underscore the importance of exact solutions. As shown in Appendix B, the determinant expression of $\langle \mu | \sigma^z | \lambda \rangle$ becomes divergent when $|\lambda\rangle$ represents string states with zero deviation due to the failure of regularization. Therefore, assuming $d_{j,\alpha}^n = 0$ may not be appropriate for our subsequent TS³A approach. Therefore, the practical route is to consider string states with finite $d_{j,\alpha}^n$.

IV. TRUNCATED STRING STATE SPACE APPROACH

In many physical problems, our focus is on the low-energy subspace rather than the entire Hilbert space [71–73]. In this study, we employ the TS³A method, as illustrated in Fig. 1(f), to gain insights into the low-energy physics of nonintegrable Heisenberg models [Eq. (2)]. The detailed construction is as follows.

When considering a nonintegrable perturbation, such as H' [Eq. (3)], the Bethe string state is no longer the eigenstate. Therefore, it becomes necessary to find the new ground state and low-energy excited states before conducting any calculations of physical quantities, such as correlation functions. The first step is to construct the matrix representation of the nonintegrable Hamiltonian H [Eq. (2)] within a truncated low-energy subspace of Bethe string states, denoted as $H_{ab}^{\text{tr}} = \delta_{ab} E_a^B + \langle B_a | H' | B_b \rangle$, with $E_a^B \leq E_{\text{cut}}^B$. The truncated dimension of H_{ab}^{tr} is typically much less than 2^N , which is determined by the energy cutoff E_{cut}^B and types of Bethe string states $|B_a\rangle$. Following the diagonalization of H^{tr} , a new ground state |GS) and low-energy excited states are obtained, which are considered to be approximate eigenstates of the Hamiltonian H .

However, an immediate question arises: How do we select the types of Bethe string states and determine the energy cutoff? To answer the first question, we investigate the form factor between Bethe string states. It is evident from Fig. 2(a) that the form factors for string states generally diminish rapidly as the difference in string length increases. For instance, the ground state of H_0 [Eq. (1)] is a 1-string state, and then we can safely truncate the string state space into relevant subspace in terms of string lengths. For the second issue, we study the asymptotic behavior of ground state energy E_{GS} and

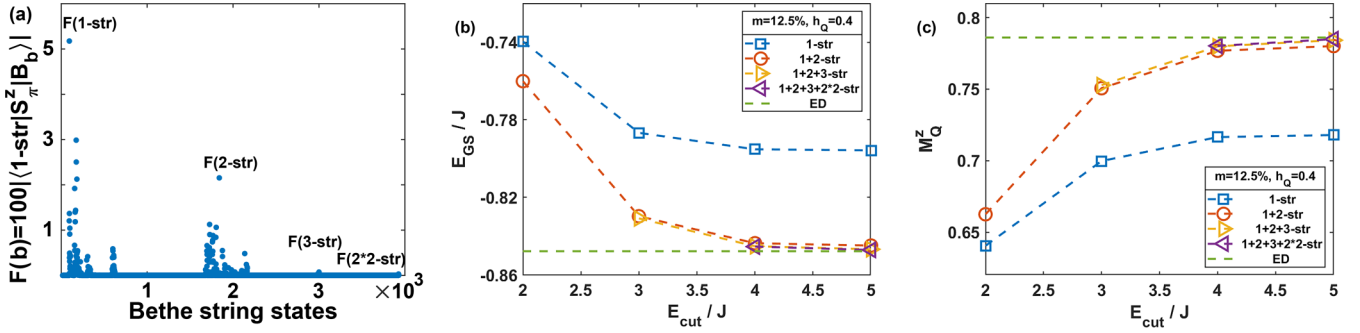


FIG. 2. (a) The absolute value of matrix entry $\langle 1\text{-str} | S_\pi^z | B_b \rangle$, where Bethe string state $|B_b\rangle$ ranges from 1-string to 2×2 -string states. (b) Ground state energy E_{GS} and (c) staggered magnetization M_Q^z calculated with different energy cutoffs and combinations of string states at $N = 16$, depicted by dashed lines with symbols. Note that the gaps of 3- and 2×2 -string states are $\simeq 2.88J$ and $\simeq 3.61J$, respectively. The green dashed line denotes the results from exact diagonalization.

the staggered magnetization $M_Q^z = \sum_j e^{-iQj} \langle GS | S_j^z | GS \rangle / \sqrt{N}$ as the energy cutoff of the truncated space increases. In Figs. 2(b) and 2(c), the calculation includes all allowed string states within a given E_{cut} . As E_{cut} increases, the results converge rapidly and approach the exact values obtained from the ED calculation. Notably, even if only 1- and 2-string states are considered, the obtained results are already very close to the exact values, while the impact of 3- and 2×2 -string states is marginal. This phenomenon confirms the suggestion that the relevant string states primarily arise from those with small length differences, as illustrated in Fig. 2(a).

V. SPIN DYNAMICS

To investigate nonintegrable spin dynamics of H [Eq. (2)], we focus on the zero-temperature dynamical structure factor (DSF) for spin along the longitudinal (z) direction ($\hbar = 1$),

$$D^{zz}(q, \omega) = 2\pi \sum_{\mu} |\langle GS | S_q^z | \mu \rangle|^2 \delta(\omega - E_{\mu} + E_{GS}), \quad (8)$$

with q being the transfer momentum and ω being the transfer energy between the ground state $|GS\rangle$ and excited states $|\mu\rangle$, whose energies are E_{GS} and E_{μ} , respectively. In the following calculation, the eigenstates $|GS\rangle$ and $|\mu\rangle$ are obtained with the TS³A developed in Sec. IV. The form factor $\langle GS | S_q^z | \mu \rangle$ is deeply related to the form factor of Bethe string states, which can be elegantly expressed in terms of the determinant [21–23, 25, 26] (a summary is given in Appendix B).

To begin with, we investigate the TS³A results under different truncation schemes for $N = 16$, $m = 12.5\%$, and $h_Q = 0.4J$. In Figs. 3(a1)–3(a4), the DSF is calculated with different selected string types and fixed energy cutoff $E_{cut} = 5J$, showing that 1- and 2-strings are the dominant states in the spin dynamics. In Figs. 3(b1)–3(b4), the DSF is calculated with different energy cutoffs and fixed string types (including 1-, 2-, 3-, and 2×2 -strings), showing that the dynamical spectrum converges quickly as E_{cut} increases. Furthermore, we compare the DSF results at $N = 16$ obtained with the TS³A to that of the ED method [74, 75], whose results reveal remarkable agreement in Fig. 4. This excellent comparison suggests that the TS³A is a highly efficient method for studying the nonintegrable spin dynamics.

In the following, we present the DSF results obtained with the TS³A at $N = 48$. Due to the staggered field perturbation term H' [Eq. (3)], where $\sum_n \cos(Qr_n) S_n^z \propto (S_Q^z + S_{-Q}^z)$, the nonvanishing matrix element of H' appears only between Bethe states with momentum difference $\Delta q = \pm Q$. As a result, the ground state consists of Bethe states with momenta nQ ($|n| = 0, 1, 2, \dots$). For static structure factor $D^{zz}(q, \omega = 0)$, a series of staggered-field-induced peaks appears at nQ ($|n| = 1, 2, \dots$), manifesting the presence of multi- Q Bethe states in the ground state. For instance, in Figs. 5(a)–5(d), there are satellite peaks at $q = 2Q, -2Q + 2\pi$ in addition to the predominant peaks at $q = Q, -Q + 2\pi$, with $Q = (1 - m)\pi$.

In Fig. 6, when $h_Q = 0$, the dynamical spectra exhibit gapless excitations at $q = (1 \pm m)\pi$, and the 2-string states are barely separated from the broad continuum of 1-string states. When $h_Q > 0$, an energy gap emerges both near the elastic line and between the continua of 1- and 2-string states. This phenomenon arises because the staggered field acts as a confining field for the Heisenberg spin chains, effectively restricting the motion of spins [43, 44, 76–78]. These induced gaps reflect the energy cost of the excitation of Bethe strings, which is known as the confinement of Bethe strings. At small magnetization [Figs. 6(a1)–6(a3)], 2-string states are effectively confined and become separated from the 1-string continuum. However, as magnetization m increases, the 2-string continuum gradually dissipates into higher energy ranges.

Notably, the capability of larger size calculations of the TS³A not only reduces the finite size effect but also renders the characteristics of the spectra more transparent and discernible. And the TS³A offers two key advantages compared to the ED method: First, it has higher efficiency, facilitating much larger systems ($N \gtrsim 50$); second, it naturally provides a unified Bethe-string-based physical picture for understanding the underlying physics.

We conclude this section by emphasizing that our model and findings offer a direct application to comprehending the low-energy spin dynamics observed in the quasi-1D antiferromagnet YbAlO₃ [58, 59, 61]. In this material, the low-energy effective Hamiltonian is described by the 1D Heisenberg models [Eq. (1)] and by Eq. (2) if the material is 3D ordered. In Fig. 5(e), the quasielastic signals obtained from neutron

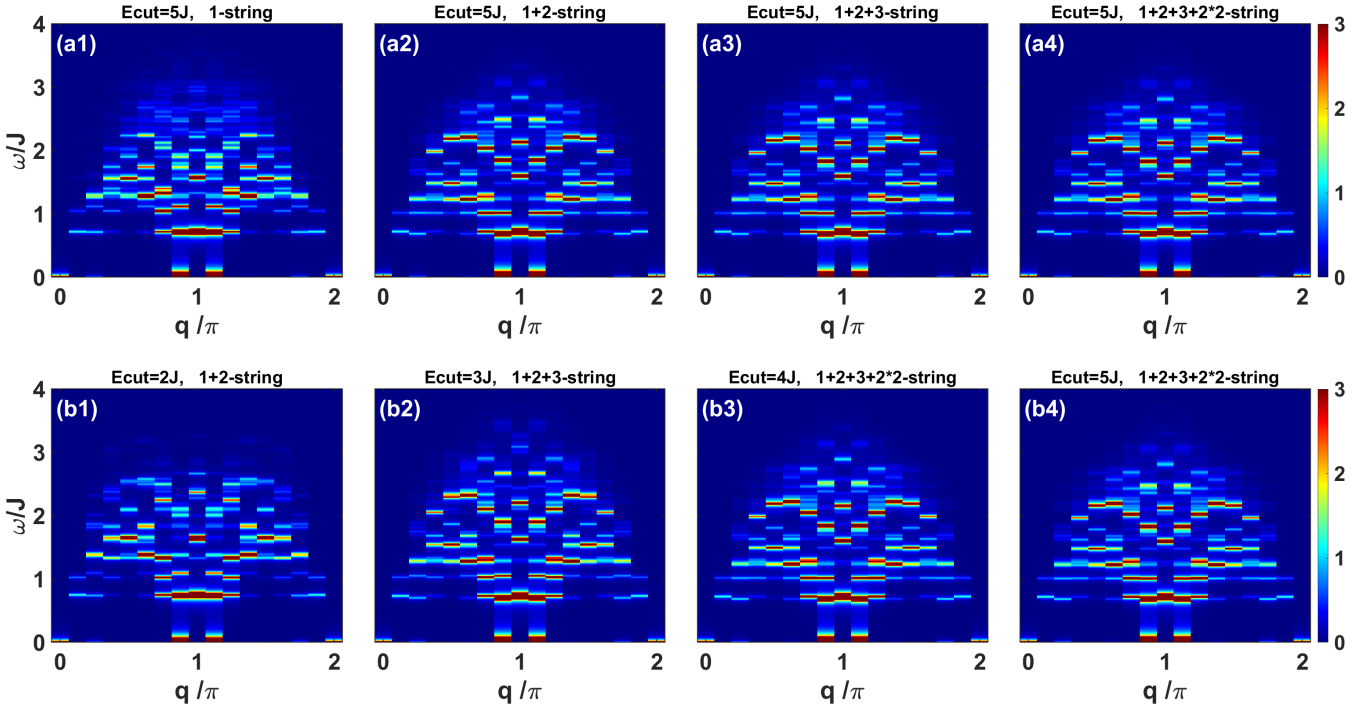


FIG. 3. Zero-temperature DSF D^z at $N = 16$, $m = 12.5\%$, $h_Q = 0.4J$ under different truncation schemes: (a1)–(a4) Different selected string types with fixed energy cutoff $E_{\text{cut}} = 5J$. (b1)–(b4) Different energy cutoffs with 1-, 2-, 3-, and 2×2 -string states. Note that the gap of 3- and 2×2 -string states are $\simeq 2.88J$ and $\simeq 3.61J$, respectively. The δ function in the DSF is broadened via the Lorentzian function $\frac{1}{\pi} \gamma / [(\omega - E_\mu + E_{\text{GS}}) + \gamma^2]$, with $\gamma = 0.02$.

scattering align with the theoretical predictions, providing compelling evidence of the coexistence of multi- Q Bethe states in the ordered phase of YbAlO_3 . Moreover, the staggered field, arising from the 3D ordering, plays the role of a confining field coupled with the spin chains within the material. As a result, the distinctive features characterizing the confined string states are observed through the inelastic neutron scattering spectra of YbAlO_3 [58].

VI. CONCLUSION

We exploited an efficient routine to find exact solutions for the Bethe string states from the BAE of the spin- $\frac{1}{2}$ Heisenberg spin chain. Based on the exact solutions we further developed the TS³A, which enabled us to determine eigenstates and eigenenergies of nonintegrable spin- $\frac{1}{2}$ Heisenberg systems with U(1) symmetry preserved. The method was then applied to systematically study the spin dynamics of the spin- $\frac{1}{2}$ Heisenberg spin chain under staggered field. In the dynamical spectra, we revealed a series of elastic peaks located at the integer multiples of the ordering wave vector Q , signifying the existence of multi- Q Bethe string states within the ground state. Moreover, the staggered field serves as a confining field for Bethe string states, inducing confinement gaps between the continua of 1- and 2-string states.

Our TS³A machine offers a Bethe-string-based scenario, contributing to a more comprehensive understanding of Heisenberg spin systems. We have demonstrated the efficiency and validity of this framework by interpreting experimental observations of the quasi-1D antiferromagnet YbAlO_3 . This intriguing consistency between theoretical

predictions based on the TS³A and experimental results motivates its extended application to ladder and two-dimensional Heisenberg systems. This broadening of scope not only enhances the versatility of the Bethe string picture but also transcends its conventional one-dimensional limitations.

ACKNOWLEDGMENTS

We thank Y. Jiang for helpful discussion. This work is supported by the National Natural Science Foundation of China under Grant No. 12274288, the Innovation Program for Quantum Science and Technology under Grant No. 2021ZD0301900, and the Natural Science Foundation of Shanghai under Grant No. 20ZR1428400.

APPENDIX A: ITERATIVE METHOD FOR EXACT SOLUTION

This Appendix presents the iterative method for solving the Bethe equation. Note that it is sufficient to solve the highest-weight state containing only finite rapidities, while other states can be obtained by adding infinite rapidities [54].

1. Deviation $d_{j,\alpha}^n = 0$

For the 1-string state, all rapidities are real, which can be directly solved with the iterative form of the Bethe equation,

$$\lambda_j = \frac{1}{2} \tan \left[\frac{\pi}{N} I_j + \frac{1}{N} \sum_{k=1}^M \arctan(\lambda_j - \lambda_k) \right], \quad (\text{A1})$$

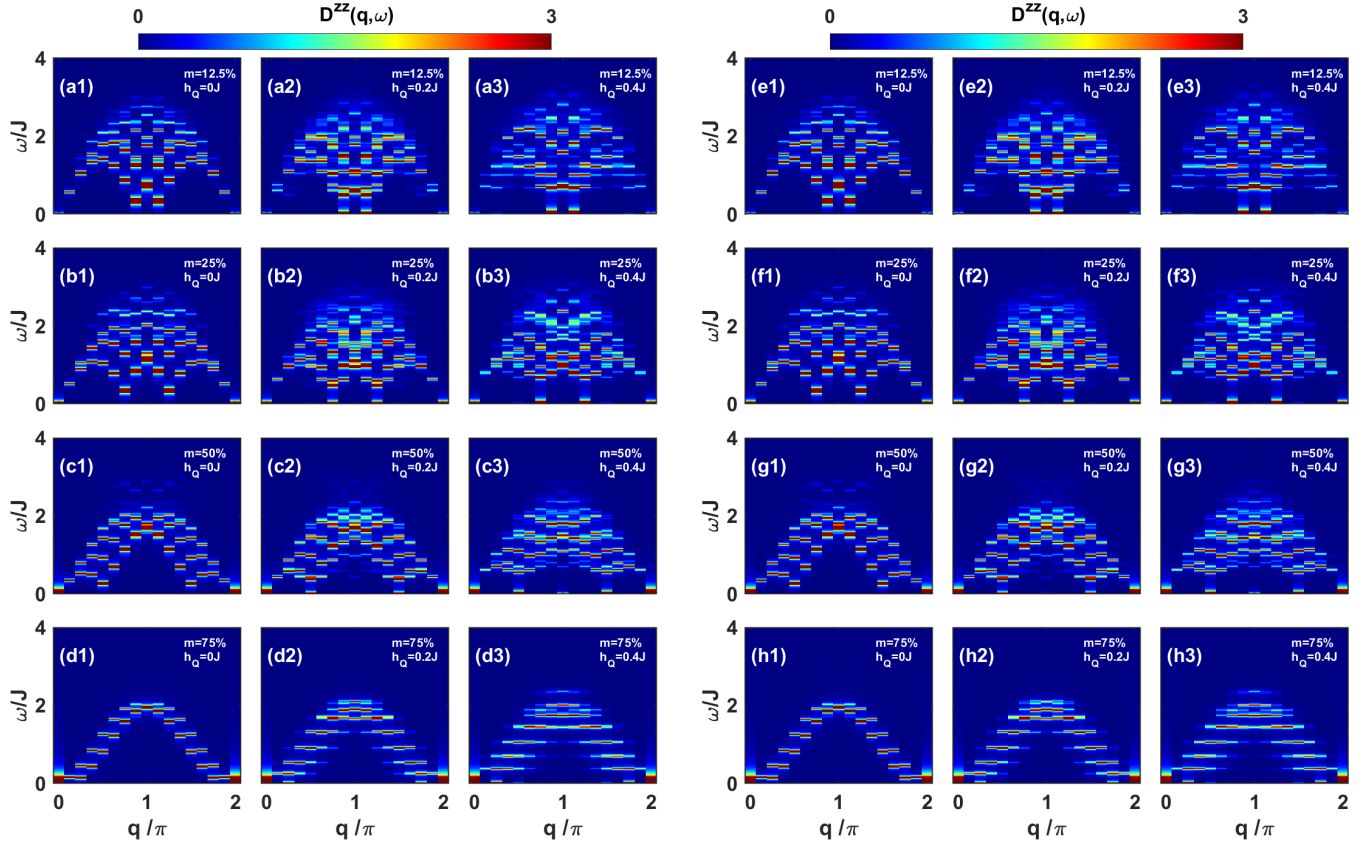


FIG. 4. Zero-temperature DSF $D^z(q, \omega)$ with different magnetizations m and staggered fields h_Q with lattice site $N = 16$. (a1)–(d3) The results obtained with TS³A consider the string types, including 1-, 2-, 3-, and 2×2 -string states with fixed energy cutoff $E_{\text{cut}} = 5J$. (e1)–(h3) ED results with the same lattice size. The δ function in the DSF is broadened via the Lorentzian function $\frac{1}{\pi} \gamma / [(\omega - E_\mu + E_{\text{GS}}) + \gamma^2]$, with $\gamma = 0.02$.

where $\{I_j\}$ is the corresponding Bethe quantum number for $\{\lambda_j\}$.

For the string state, there is at least one complex rapidity in the pattern of Eq. (5). To obtain the corresponding rapidities, we convert the reduced Bethe equation (7) into the iterative form,

$$\lambda_{j,\alpha} = \frac{j}{2} \tan \left[\frac{\pi}{N} I_{j,\alpha} + \frac{1}{2N} \sum_{k=1}^M \sum_{\beta=1}^{M_k} \Theta_{jk}(\lambda_{j,\alpha} - \lambda_{k,\beta}) \right], \quad (A2)$$

where $\{I_{j,\alpha}\}$ is the corresponding reduced Bethe quantum number for string centers $\{\lambda_{j,\alpha}\}$. Following Eq. (5), the complex string states is constructed from $\{\lambda_{j,\alpha}\}$ with $d_{j,\alpha}^n = 0$.

2. Deviation $d_{j,\alpha}^n \neq 0$

To determine the exact deviation $\{d_{j,\alpha}^n\}$, the strategy becomes more intricate for the XXX model [54] and for the gapped XXZ model [26]. Here, we consider only 2- and 3-string states for illustration.

For a string with length $j = 2$, its two complex rapidities are $\lambda_j^{+,-} = \lambda_j^0 \pm \frac{i}{2} + d_j^{1,2}$, where the deviations are purely imaginary, $d_j^1 = i\delta_j^1$ and $d_j^2 = i\delta_j^2 = -i\delta_j^1$. Then we

have the first-order deviation,

$$\delta_{j=2}^1 \approx \left(\frac{\lambda_j^+ - i/2}{\lambda_j^+ + i/2} \right)^N \left(\prod_k^{\text{real}} \frac{\lambda_j^+ - \lambda_k + i}{\lambda_j^+ - \lambda_k - i} \right). \quad (A3)$$

Next, utilizing the first-order deviation, we can determine the true Bethe quantum number $J^{1,2}$ from the reduced one I_2 ,

$$J^1 = J^2 - \Theta_H(\delta) = \frac{1}{2} \left(I_2 + \frac{N}{2} \text{sgn}(\lambda_j^0) - \Theta_H(\delta) \right), \quad (A4)$$

where

$$\Theta_H(\delta) = \frac{N}{2} - M + 1 + I_2 \pmod{2}. \quad (A5)$$

Then, considering the sum of the logarithmic Bethe equation (6),

$$\sum_{\sigma \in \{+, -\}} \Theta_1(\lambda^\sigma) = \frac{1}{N} \sum_{\sigma \in \{+, -\}} \left(2\pi I_\sigma + \sum_{k=1}^M \Theta_2(\lambda^\sigma - \lambda_k) \right), \quad (A6)$$

and the deformation of Bethe equation (4),

$$\frac{\lambda^+ - \lambda^- - i}{\lambda^+ - \lambda^- + i} = \left(\frac{\lambda^+ - i/2}{\lambda^+ + i/2} \right)^N \prod_k \frac{\lambda^+ - \lambda_k + i}{\lambda^+ - \lambda_k - i}, \quad (A7)$$

we can solve for λ^\pm , along with $\{\lambda_1\}_{M-2}$ from the Bethe equation (6) for 1-strings.

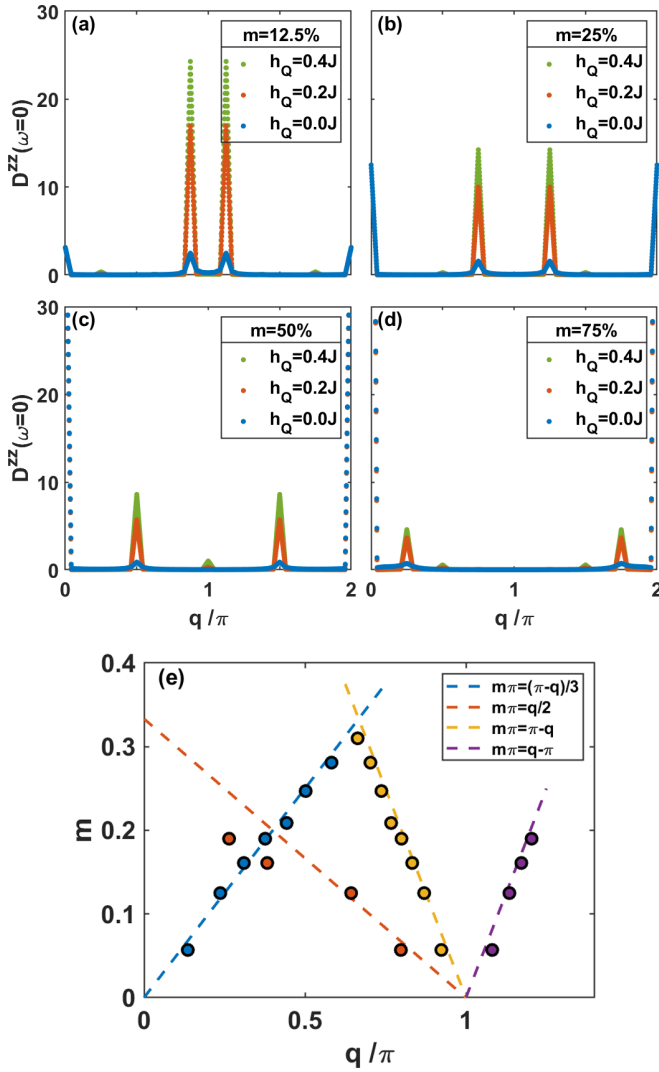


FIG. 5. (a)–(d) The static structure factor $D^{zz}(\omega = 0)$ with $N = 48$; $h_Q = 0J, 0.2J$, and $0.4J$; and magnetization density $m = 12.5\%$, 25% , 50% , 75% , obtained with the TS³A. (e) Comparison between experimental data (solid circles) and theoretical predictions (dashed lines). The solid circles represent satellite peaks obtained from quasielastic neutron scattering data, extracted from Ref. [61]. The dashed lines represent the theoretical prediction for the elastic peaks.

For a string with length $j = 3$, it contains three rapidities, $\lambda_j^0, \lambda_j^{+, -} = \lambda_j^{1,2} = \lambda_j^0 \pm i + d_j^{1,2}$, where $d_j^1 = (d_j^2)^* = \epsilon^1 + i\delta^1$. Then we have the first-order deviation,

$$d_{j=3}^1 \approx 6i \left(\frac{\lambda_j^1 + i/2}{\lambda_j^1 - i/2} \right)^{-N} \left(\prod_k^{\text{real}} \frac{\lambda_j^1 - \lambda_k + i}{\lambda_j^1 - \lambda_k - i} \right). \quad (\text{A8})$$

We note that for the 3-string, $\text{Im}(\lambda^+) > 1/2$ must hold, which leads to the fact that J^\pm must be a wide pair with $J^- - J^+ = 1$. Then, we still need two more equations to solve the true Bethe quantum numbers J^0 and J^\pm . The first equation is the sum of the logarithmic Bethe Eq. (6),

$$J^+ + J^0 + J^- = I_3 - \frac{1}{2} \sum_{k=1}^{\text{1-str}} \text{sgn}(\lambda - \lambda_k). \quad (\text{A9})$$

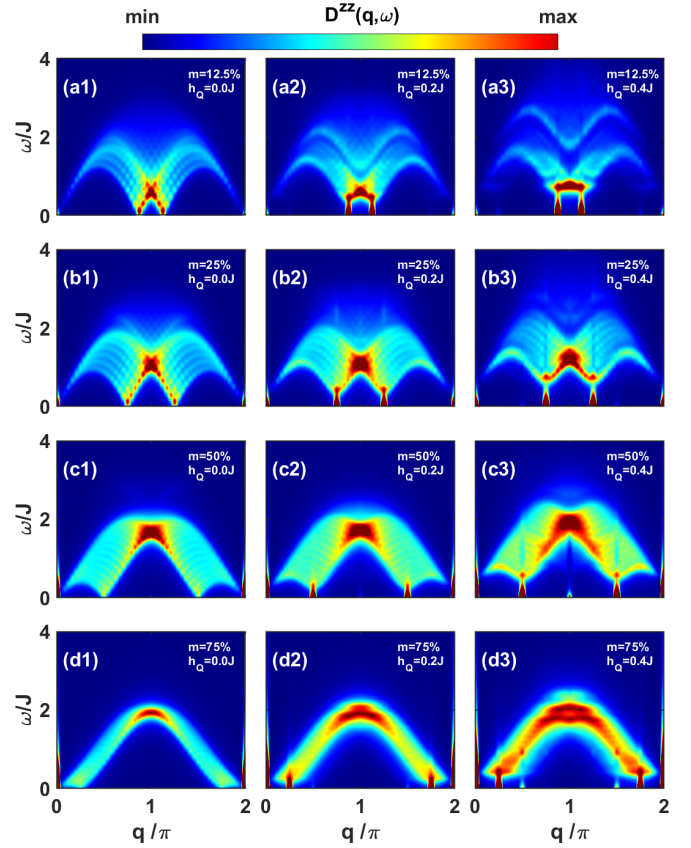


FIG. 6. Zero-temperature DSF $D^{zz}(q, \omega)$ with $N = 48$ obtained with the TS³A. The DSFs have $h_Q = 0J, 0.2J$, and $0.4J$ (from left to right) and magnetization density $m = 12.5\%$, 25% , 50% , 75% (from top to bottom). The δ function in the DSF is broadened via the Lorentzian function $\frac{1}{\pi} \gamma / [(\omega - E_\mu + E_{GS}) + \gamma^2]$, with $\gamma = 0.12$. The data are further interpolated along the horizontal direction for 800 query points with equal spacing.

Another necessary equation is the sum of logarithmic BAEs of λ^\pm ,

$$\begin{aligned} 2\pi(J^+ + J^-) + \Theta_2(\lambda^+ - \lambda^0) + \Theta_2(\lambda^- - \lambda^0) \\ = N[\Theta_1(\lambda^+) + \Theta_1(\lambda^-)] - \Theta_2(\lambda^+ - \lambda^-) - \Theta_2(\lambda^- - \lambda^+) \\ - \sum_{k=1, \beta} [\Theta_2(\lambda^+ - \lambda_{k, \beta}) + \Theta_2(\lambda^- - \lambda_{k, \beta})]. \end{aligned} \quad (\text{A10})$$

Let A be the right-hand side of Eq. (A10). Because $\Theta_2(\lambda^+ - \lambda^0) + \Theta_2(\lambda^- - \lambda^0) \in (-2\pi, 2\pi)$, $J^+ + J^-$ is the even (odd) integer number in $(A/2\pi - 1, A/2\pi + 1)$ when M is even (odd). Therefore,

$$\begin{aligned} J^+ + J^- = [1 + (-1)^M] \left[\frac{1}{2} \left(\frac{A}{2\pi} + 1 \right) \right] \\ + [1 - (-1)^M] \left[\left[\frac{1}{2} \left(\frac{A}{2\pi} + 1 \right) + \frac{1}{2} \right] - \frac{1}{2} \right]. \end{aligned} \quad (\text{A11})$$

Now combining the wide pair condition ($J^- - J^+ = 1$), Eqs. (A9) and (A11), J^\pm and J^0 can be determined. The Bethe quantum number (BQN) $\{J_k\}$ for real rapidities can be shown

TABLE II. The solutions of a 3-string state of the Bethe ansatz equation (4) with $N = 12$ and $M = 5$. The unphysical solutions with repeated rapidities are obtained with the method described in Secs. A 1 and A 2. The physical solutions are obtained with the method described in Sec. A 3.

	$\{J\}_{M=5}$	$\{I\}_{M=5}$	$\{\lambda\}_{M=5}$	Energy
Unphysical	4		$0.495521913637784 + 0.962224932131036i$	-3.632275481625215
	3	1_3	$0.445792844757107 + 0.000000000000000i$	
	5		$0.495521913637784 - 0.962224932131036i$	
	2	$3/2_1$	$0.180317318693691 + 0.000000000000000i$	
	3	$5/2_1$	$0.445792844757134 + 0.000000000000000i$	
Physical	4		$0.491814213695900 + 0.961471132379077i$	-3.60069325626932
	3	1_3	$0.444763506448628 + 0.018770199402376i$	
	5		$0.491814213695898 - 0.961471132379085i$	
	2	$3/2_1$	$0.180714318631831 + 0.000000000000000i$	
	3	$5/2_1$	$0.444763506448649 - 0.018770199402378i$	

to have the following expression:

$$J_k = I_k - \frac{1}{2} \text{sgn}(\lambda_k - \lambda_{j=3}^0). \quad (\text{A12})$$

To solve rapidities, we first need the sum of the logarithmic BAE of J^\pm and J^0 without setting ϵ and δ to zero:

$$\begin{aligned} \frac{2\pi}{N}(J^+ + J^0 + J^-) &= \Theta_1(\lambda^+) + \Theta_1(\lambda^0) + \Theta_1(\lambda^-) \\ &- \frac{1}{N} \sum_k^{\text{real}} \Theta_2(\lambda^+ - \lambda_k) + \Theta_2(\lambda^0 - \lambda_k) + \Theta_2(\lambda^- - \lambda_k). \end{aligned} \quad (\text{A13})$$

The second equation is the sum of the logarithmic BAE of J^\pm [Eq. (A10)]. The third one is obtained from Bethe equation (4) after some simple manipulation,

$$\begin{aligned} \frac{(\lambda^+ - \lambda^0) - i}{(\lambda^+ - \lambda^0) + i} &= \frac{(\lambda^+ - \lambda^-) + i}{(\lambda^+ - \lambda^-) - i} \prod_k \frac{(\lambda^+ - \lambda_k) + i}{(\lambda^+ - \lambda_k) - i} \\ &\times \left(\frac{\lambda^+ - i/2}{\lambda^+ + i/2} \right)^N. \end{aligned} \quad (\text{A14})$$

The logarithmic Bethe equation (6) is also needed for real rapidities.

Here, we present the 3-string state results with $N = 12$ and $M = 5$ obtained from the above iterative method in the unphysical set in Table II. We observe that two real rapidities coincide; one is the string center, and the other is a 1-string. However, it is unphysical because of the incorrect eigenenergy and the absence of a wave function in this set of solutions.

3. Repeated real rapidities

To tackle the issue of the repeated real rapidities of λ^0 , we introduce a small imaginary part to create a complex-conjugate pair, as required by the BAE. Now, we have two complex-conjugate pairs. The first pair has a small imaginary part, $\lambda^{0\pm} = \lambda_0 \pm i\delta_0$, while the second one has a larger imaginary part around $\pm i$, $\lambda^{3\pm} = \lambda_3 \pm i(1 + \delta_3)$. Note that four complex rapidities need four equations to solve. The strategy is similar to the procedures mentioned above. Two equations come from the sum of logarithmic Bethe equations of $\lambda^{0\pm}$ and $\lambda^{3\pm}$. Another two equations come from the original Bethe equations of λ^{0+} and λ^{3+} . Combining the logarithmic

Bethe equations for real rapidity, we can solve $\lambda^{0\pm}$, $\lambda^{3\pm}$, and real rapidities $\{\lambda_1\}_{M=4}$.

Then, we redetermine the 3-string state for $N = 12$ and $M = 5$ (in the physical set in Table II). Now, this set of rapidities is the exact solution of the original Bethe equation (4), which is consistent with Ref. [69], the rational Q -system method, and the ED calculation.

APPENDIX B: THE DETERMINANT FORMULA

1. Norm of the Bethe state

Given a set of rapidities λ_j ($j = 1, \dots, M$) representing exact solutions of the Bethe ansatz equation (4), the norm of the corresponding Bethe state is expressed as [2,54,79]

$$\mathbb{N}_M(\{\lambda_j\}) = (-1)^M \frac{\prod_{j \neq k} (\lambda_j - \lambda_k + i)}{\prod_{j \neq k} (\lambda_j - \lambda_k)} \det \Phi(\{\lambda\}), \quad (\text{B1})$$

where the matrix elements of Φ are

$$\begin{aligned} \Phi_{ab} &= \delta_{ab} \left[N \frac{4}{1 + 4\lambda_a^2} - \sum_k \frac{2}{1 + (\lambda_a - \lambda_k)^2} \right] \\ &+ (1 - \delta_{ab}) \frac{2}{1 + (\lambda_a - \lambda_b)^2}. \end{aligned} \quad (\text{B2})$$

2. Form factors

The nonzero form factors associated with σ^z correspond to states characterized by equal magnon numbers,

$$\begin{aligned} F_j^z(\{\mu\}_M, \{\lambda\}_M) &= \langle \{\mu\}_M | \sigma_j^z | \{\lambda\}_M \rangle \\ &= \frac{\phi_{j-1}(\{\mu\}_M)}{\phi_{j-1}(\{\lambda\}_M)} \prod_{l=1}^M \frac{(\mu_l + i/2)}{(\lambda_l + i/2)} \\ &\times \frac{i^M \det(H - 2P)}{\prod_{l>m} (\mu_l - \mu_m) \prod_{l<m} (\lambda_l - \lambda_m)}, \end{aligned} \quad (\text{B3})$$

where $\phi_j(\{\lambda\}_M) = e^{-iq_\lambda r_j}$ and q_λ is the eigenmomentum of the Bethe state $|\{\lambda\}_M\rangle$. The matrix elements of the H and P matrices are defined as

$$H_{ab} = \frac{1}{(\mu_a - \lambda_b)} \left[\prod_{l \neq a}^M (\mu_l - \lambda_b + i) - \left(\frac{\lambda_b - i/2}{\lambda_b + i/2} \right)^N \prod_{l \neq a}^M (\mu_l - \lambda_b - i) \right], \quad (\text{B4})$$

$$P_{ab} = \frac{\prod_{l=1}^M (\lambda_l - \lambda_b + i)}{(\mu_a + i/2)(\mu_a - i/2)}, \quad (\text{B5})$$

respectively. Here, we note that both the 2- and 3-string states with $d_{j,\alpha}^n = 0$ can cause divergence in the P matrix (B5). However, the divergence cannot be regularized since there are no common terms in the H matrix (B4).

-
- [1] M. Jimbo and T. Miwa, *Algebraic Analysis of Solvable Lattice Models* (American Mathematical Society, Providence, RI, 1995).
- [2] F. Franchini, *An Introduction to Integrable Techniques for One-Dimensional Quantum Systems*, Lecture Notes in Physics Vol. 940 (Springer, Cham, 2017).
- [3] J. Yang, X. Wang, and J. Wu, Magnetic excitations in the one-dimensional Heisenberg-Ising model with external fields and their experimental realizations, *J. Phys. A* **56**, 013001 (2023).
- [4] F. He, Y. Jiang, Y.-C. Yu, H.-Q. Lin, and X.-W. Guan, Quantum criticality of spinons, *Phys. Rev. B* **96**, 220401(R) (2017).
- [5] M. Gaudin, Un système à une dimension de fermions en interaction, *Phys. Lett. A* **24**, 55 (1967).
- [6] C. N. Yang, Some exact results for the many-body problem in one dimension with repulsive delta-function interaction, *Phys. Rev. Lett.* **19**, 1312 (1967).
- [7] X.-W. Guan, M. T. Batchelor, and C. Lee, Fermi gases in one dimension: From Bethe ansatz to experiments, *Rev. Mod. Phys.* **85**, 1633 (2013).
- [8] E. H. Lieb and W. Liniger, Exact analysis of an interacting Bose gas. I. The general solution and the ground state, *Phys. Rev.* **130**, 1605 (1963).
- [9] E. H. Lieb, Exact analysis of an interacting Bose gas. II. The excitation spectrum, *Phys. Rev.* **130**, 1616 (1963).
- [10] P. Pfeuty, The one-dimensional Ising model with a transverse field, *Ann. Phys. (NY)* **57**, 79 (1970).
- [11] T. Niemeijer, Some exact calculations on a chain of spins 1/2, *Physica (Amsterdam)* **36**, 377 (1967).
- [12] D. Boyanovsky, Field theory of the two-dimensional Ising model: Conformal invariance, order and disorder, and bosonization, *Phys. Rev. B* **39**, 6744 (1989).
- [13] A. B. Zamolodchikov, Integrables of motion and S-matrix of the (scaled) $T = T_c$ Ising model with magnetic field, *Int. J. Mod. Phys. A* **04**, 4235 (1989).
- [14] R.-T. Li, S. Cheng, Y.-Y. Chen, and X.-W. Guan, Exact results of dynamical structure factor of Lieb-Liniger model, *J. Phys. A* **56**, 335204 (2023).
- [15] H. Guan and N. Andrei, Quench dynamics of the Gaudin-Yang model, [arXiv:1803.04846](https://arxiv.org/abs/1803.04846).
- [16] N. Kitanine, J. M. Maillet, and V. Terras, Form factors of the XXZ Heisenberg spin-1/2 finite chain, *Nucl. Phys. B* **554**, 647 (1999).
- [17] N. Kitanine, J. M. Maillet, and V. Terras, Correlation functions of the XXZ Heisenberg spin-1/2 chain in a magnetic field, *Nucl. Phys. B* **567**, 554 (2000).
- [18] J. Yang, W. Yuan, T. Imai, Q. Si, J. Wu, and M. Kormos, Local dynamics and thermal activation in the transverse-field Ising chain, *Phys. Rev. B* **106**, 125149 (2022).
- [19] N. Iorgov, V. Shadura, and Y. Tykhyy, Spin operator matrix elements in the quantum Ising chain: Fermion approach, *J. Stat. Mech.* (2011) P02028.
- [20] G. Mussardo, *Statistical Field Theory: An Introduction to Exactly Solved Models in Statistical Physics* (Oxford University Press, Oxford, 2020).
- [21] J.-S. Caux and R. Hagemans, The four-spinon dynamical structure factor of the Heisenberg chain, *J. Stat. Mech.* (2006) P12013.
- [22] J.-S. Caux, J. Mossel, and I. P. Castillo, The two-spinon transverse structure factor of the gapped Heisenberg antiferromagnetic chain, *J. Stat. Mech.* (2008) P08006.
- [23] I. P. Castillo, The exact two-spinon longitudinal dynamical structure factor of the anisotropic XXZ model, [arXiv:2005.10729](https://arxiv.org/abs/2005.10729).
- [24] M. Takahashi, One-dimensional Heisenberg model at finite temperature, *Prog. Theor. Phys.* **46**, 401 (1971).
- [25] M. Kohno, Dynamically dominant excitations of string solutions in the spin-1/2 antiferromagnetic Heisenberg chain in a magnetic field, *Phys. Rev. Lett.* **102**, 037203 (2009).
- [26] W. Yang, J. Wu, S. Xu, Z. Wang, and C. Wu, One-dimensional quantum spin dynamics of Bethe string states, *Phys. Rev. B* **100**, 184406 (2019).
- [27] R. Coldea, D. A. Tennant, E. M. Wheeler, E. Wawrzynska, D. Prabhakaran, M. Telling, K. Habicht, P. Smeibidl, and K. Kiefer, Quantum criticality in an Ising chain: Experimental evidence for emergent E_8 symmetry, *Science* **327**, 177 (2010).
- [28] J. Wu, M. Kormos, and Q. Si, Finite-temperature spin dynamics in a perturbed quantum critical Ising chain with an E_8 symmetry, *Phys. Rev. Lett.* **113**, 247201 (2014).
- [29] X. Wang, H. Zou, K. Hódsági, M. Kormos, G. Takács, and J. Wu, Cascade of singularities in the spin dynamics of a perturbed quantum critical Ising chain, *Phys. Rev. B* **103**, 235117 (2021).
- [30] H. Zou, Y. Cui, X. Wang, Z. Zhang, J. Yang, G. Xu, A. Okutani, M. Hagiwara, M. Matsuda, G. Wang, G. Mussardo, K. Hódsági, M. Kormos, Z. He, S. Kimura, R. Yu, W. Yu, J. Ma, and J. Wu, E_8 spectra of quasi-one-dimensional antiferromagnet $\text{BaCo}_2\text{V}_2\text{O}_8$ under transverse field, *Phys. Rev. Lett.* **127**, 077201 (2021).
- [31] X. Wang, K. Puzniak, K. Schmalzl, C. Balz, M. Matsuda, A. Okutani, M. Hagiwara, J. Ma, J. Wu, and B. Lake, Spin dynamics of the e_8 particles, [arXiv:2308.00249](https://arxiv.org/abs/2308.00249).

- [32] Y. Gao, X. Wang, N. Xi, Y. Jiang, R. Yu, and J. Wu, Spin dynamics and dark particle in a weak-coupled quantum Ising ladder with $\mathcal{D}_8^{(1)}$ spectrum, [arXiv:2402.11229](#).
- [33] N. Xi, X. Wang, Y. Gao, Y. Jiang, R. Yu, and J. Wu, Emergent $\mathcal{D}_8^{(1)}$ spectrum and topological soliton excitation in CoNb_2O_6 , [arXiv:2403.10785](#).
- [34] A. LeClair, A. Ludwig, and G. Mussardo, Integrability of coupled conformal field theories, *Nucl. Phys. B* **512**, 523 (1998).
- [35] B. Lake, D. A. Tennant, J.-S. Caux, T. Barthel, U. Schollwöck, S. E. Nagler, and C. D. Frost, Multispinon continua at zero and finite temperature in a near-ideal Heisenberg chain, *Phys. Rev. Lett.* **111**, 137205 (2013).
- [36] Z. Wang, J. Wu, W. Yang, A. K. Bera, D. Kamenskyi, A. T. M. N. Islam, S. Xu, J. M. Law, B. Lake, C. Wu, and A. Loidl, Experimental observation of Bethe strings, *Nature (London)* **554**, 219 (2018).
- [37] A. K. Bera, J. Wu, W. Yang, R. Bewley, M. Boehm, J. Xu, M. Bartkowiak, O. Prokhnenko, B. Klemke, A. T. M. N. Islam, J. M. Law, Z. Wang, and B. Lake, Dispersions of many-body Bethe strings, *Nat. Phys.* **16**, 625 (2020).
- [38] Z. Wang, M. Schmidt, A. Loidl, J. Wu, H. Zou, W. Yang, C. Dong, Y. Kohama, K. Kindo, D. I. Gorbunov, S. Niesen, O. Breunig, J. Engelmayer, and T. Lorenz, Quantum critical dynamics of a Heisenberg-Ising chain in a longitudinal field: Many-body strings versus fractional excitations, *Phys. Rev. Lett.* **123**, 067202 (2019).
- [39] Z. Zhang, K. Amelin, X. Wang, H. Zou, J. Yang, U. Nagel, T. Rößm, T. Dey, A. A. Nugroho, T. Lorenz, J. Wu, and Z. Wang, Observation of E_8 particles in an Ising chain antiferromagnet, *Phys. Rev. B* **101**, 220411(R) (2020).
- [40] K. Amelin, J. Engelmayer, J. Viirik, U. Nagel, T. Rößm, T. Lorenz, and Z. Wang, Experimental observation of quantum many-body excitations of E_8 symmetry in the Ising chain ferromagnet CoNb_2O_6 , *Phys. Rev. B* **102**, 104431 (2020).
- [41] R. Steinigeweg, J. Herbrych, X. Zotos, and W. Brenig, Heat conductivity of the Heisenberg spin- $\frac{1}{2}$ ladder: From weak to strong breaking of integrability, *Phys. Rev. Lett.* **116**, 017202 (2016).
- [42] M. T. Batchelor, X. W. Guan, N. Oelkers, and Z. Tsuboi, Integrable models and quantum spin ladders: Comparison between theory and experiment for the strong coupling ladder compounds, *Adv. Phys.* **56**, 465 (2007).
- [43] F. H. L. Essler, A. M. Tsvelik, and G. Delfino, Quasi-one-dimensional spin- $\frac{1}{2}$ Heisenberg magnets in their ordered phase: Correlation functions, *Phys. Rev. B* **56**, 11001 (1997).
- [44] O. A. Starykh and L. Balents, Excitations and quasi-one-dimensionality in field-induced nematic and spin density wave states, *Phys. Rev. B* **89**, 104407 (2014).
- [45] J. Bonča, J. P. Rodriguez, J. Ferrer, and K. S. Bedell, Direct calculation of spin stiffness for spin- $\frac{1}{2}$ Heisenberg models, *Phys. Rev. B* **50**, 3415 (1994).
- [46] F. Heidrich-Meisner, A. Honecker, D. C. Cabra, and W. Brenig, Zero-frequency transport properties of one-dimensional spin- $\frac{1}{2}$ systems, *Phys. Rev. B* **68**, 134436 (2003).
- [47] A. Keselman, L. Balents, and O. A. Starykh, Dynamical signatures of quasiparticle interactions in quantum spin chains, *Phys. Rev. Lett.* **125**, 187201 (2020).
- [48] C. Zhou, Z. Yan, H.-Q. Wu, K. Sun, O. A. Starykh, and Z. Y. Meng, Amplitude mode in quantum magnets via dimensional crossover, *Phys. Rev. Lett.* **126**, 227201 (2021).
- [49] M. Takahashi and M. Suzuki, One-dimensional anisotropic Heisenberg model at finite temperatures, *Prog. Theor. Phys.* **48**, 2187 (1972).
- [50] T. Fujita, T. Kobayashi, and H. Takahashi, Large- N behaviour of string solutions in the Heisenberg model, *J. Phys. A* **36**, 1553 (2003).
- [51] A. Ilakovac, M. Kolanović, S. Pallua, and P. Prester, Violation of the string hypothesis and the Heisenberg XXZ spin chain, *Phys. Rev. B* **60**, 7271 (1999).
- [52] K. Isler and M. B. Paranjape, Violations of the string hypothesis in the solutions of the Bethe ansatz equations in the XXX-Heisenberg model, *Phys. Lett. B* **319**, 209 (1993).
- [53] F. H. L. Essler, V. E. Korepin, and K. Schoutens, Fine structure of the Bethe ansatz for the spin- $\frac{1}{2}$ Heisenberg XXX model, *J. Phys. A* **25**, 4115 (1992).
- [54] R. Hagemans and J.-S. Caux, Deformed strings in the Heisenberg model, *J. Phys. A* **40**, 14605 (2007).
- [55] C. Marboe and D. Volin, Fast analytic solver of rational Bethe equations, *J. Phys. A* **50**, 204002 (2017).
- [56] Z. Bajnok, E. Granet, J. L. Jacobsen, and R. I. Nepomechie, On generalized Q -systems, *J. High Energy Phys.* **03** (2020) 177.
- [57] J. Hou, Y. Jiang, and R.-D. Zhu, Spin- s rational Q -system, *SciPost Phys.* **16**, 113 (2024).
- [58] J. Yang, T. Xie, S. E. Nikitin, J. Wu, and A. Podlesnyak, Confinement of many-body Bethe strings, *Phys. Rev. B* **108**, L020402 (2023).
- [59] L. S. Wu, S. E. Nikitin, Z. Wang, W. Zhu, C. D. Batista, A. M. Tsvelik, A. M. Samarakoon, D. A. Tennant, M. Brando, L. Vasylichko, M. Frontzek, A. T. Savici, G. Sala, G. Ehlers, A. D. Christianson, M. D. Lumsden, and A. Podlesnyak, Tomonaga-Luttinger liquid behavior and spinon confinement in YbAlO_3 , *Nat. Commun.* **10**, 698 (2019).
- [60] Y. Fan, J. Yang, W. Yu, J. Wu, and R. Yu, Phase diagram and quantum criticality of Heisenberg spin chains with Ising anisotropic interchain couplings, *Phys. Rev. Res.* **2**, 013345 (2020).
- [61] S. E. Nikitin, S. Nishimoto, Y. Fan, J. Wu, L. S. Wu, A. S. Sukhanov, M. Brando, N. S. Pavlovskii, J. Xu, L. Vasylichko, R. Yu, and A. Podlesnyak, Multiple fermion scattering in the weakly coupled spin-chain compound YbAlO_3 , *Nat. Commun.* **12**, 3599 (2021).
- [62] A. K. Bera, B. Lake, W.-D. Stein, and S. Zander, Magnetic correlations of the quasi-one-dimensional half-integer spin-chain antiferromagnets $\text{SrM}_2\text{V}_2\text{O}_8$ ($M = \text{Co}, \text{Mn}$), *Phys. Rev. B* **89**, 094402 (2014).
- [63] H. Bethe, Zur Theorie der Metalle, *Z. Phys.* **71**, 205 (1931).
- [64] M. Karabach, G. Müller, H. Gould, and J. Tobochnik, Introduction to the Bethe ansatz I, *Comput. Phys.* **11**, 36 (1997).
- [65] M. Karbach, K. Hu, and G. Müller, Introduction to the Bethe ansatz III, [arXiv:cond-mat/0008018](#).
- [66] A. A. Vladimirov, Proof of the invariance of the Bethe-ansatz solutions under complex conjugation, *Theor. Math. Phys.* **66**, 102 (1986).
- [67] M. Takahashi, *Thermodynamics of One-Dimensional Solvable Models* (Cambridge University Press, Cambridge, 1999).
- [68] W. Press, S. Teukolsky, W. Vetterling, and B. Flannery, *Numerical Recipes in C++: The Art of Scientific*

- Computing* (Cambridge University Press, Cambridge, 2007).
- [69] T. Deguchi and P. R. Giri, Non self-conjugate strings, singular strings and rigged configurations in the Heisenberg model, *J. Stat. Mech.* (2015) P02004.
- [70] In the spin- $\frac{1}{2}$ XXX chain, we can check this invalidity by inserting the unphysical solutions into the wave function.
- [71] A. J. A. James, R. M. Konik, P. Lecheminant, N. J. Robinson, and A. M. Tsvelik, Non-perturbative methodologies for low-dimensional strongly-correlated systems: From non-Abelian bosonization to truncated spectrum methods, *Rep. Prog. Phys.* **81**, 046002 (2018).
- [72] V. P. Yurov and A. B. Zamolodchikov, Truncated comformal space approach to scaling Lee-Yang model, *Int. J. Mod. Phys. A* **5**, 3221 (1990).
- [73] J.-S. Caux and R. M. Konik, Constructing the generalized Gibbs ensemble after a quantum quench, *Phys. Rev. Lett.* **109**, 175301 (2012).
- [74] H. Q. Lin, Exact diagonalization of quantum-spin models, *Phys. Rev. B* **42**, 6561 (1990).
- [75] J.-H. Jung and J. D. Noh, Guide to exact diagonalization study of quantum thermalization, *J. Korean Phys. Soc.* **76**, 670 (2020).
- [76] B. Lake, A. M. Tsvelik, S. Notbohm, D. Alan Tennant, T. G. Perring, M. Reehuis, C. Sekar, G. Krabbes, and B. Büchner, Confinement of fractional quantum number particles in a condensed-matter system, *Nat. Phys.* **6**, 50 (2010).
- [77] A. K. Bera, B. Lake, F. H. L. Essler, L. Vanderstraeten, C. Hubig, U. Schollwöck, A. T. M. N. Islam, A. Schneidewind, and D. L. Quintero-Castro, Spinon confinement in a quasi-one-dimensional anisotropic Heisenberg magnet, *Phys. Rev. B* **96**, 054423 (2017).
- [78] Z. Wang, J. Wu, S. Xu, W. Yang, C. Wu, A. K. Bera, A. T. M. N. Islam, B. Lake, D. Kamenskyi, P. Gogoi, H. Engelkamp, N. Wang, J. Deisenhofer, and A. Loidl, From confined spinons to emergent fermions: Observation of elementary magnetic excitations in a transverse-field Ising chain, *Phys. Rev. B* **94**, 125130 (2016).
- [79] N. A. Slavnov, Calculation of scalar products of wave functions and form factors in the framework of the algebraic Bethe ansatz, *Theor. Math. Phys.* **79**, 502 (1989).